JOURNAL OF SOLID STATE CHEMISTRY 112, 262–269 (1994)

Structural and Electronic Properties of the Dilute Magnet $Sr_{3x}La_{2-3x}Zn_{1-x}Ru_xO_4$ ($\frac{1}{3} \leq x \leq \frac{2}{3}$)

S. H. Kim and P. D. Battle[1]

Inorganic Chemistry Laboratory, South Parks Road, Oxford, OX1 3QR, United Kingdom

Received July 8, 1993; in revised form November 29, 1993; accepted December 2, 1993

The solid solution $Sr_{3x}La_{2-3x}Zn_{1-x}Ru_xO_4$ ($\frac{1}{3} \leq x \leq \frac{2}{3}$) has the tetragonal K_2NiF_4 structure with a disordered arrangement of Zn^{2+} and Ru^{5+} over the octahedral sites. The sample with $x = \frac{1}{3}$ is found to be paramagnetic over the temperature range $6 < T < 296$ K. As the ruthenium concentration increases, short-range antiferromagnetic interactions between Ru^{5+} ions become more important; the magnetic susceptibility shows a maximum at low temperatures when x is larger than the percolation threshold for a nearest-neighbor square lattice (0.59). However, the magnetic irreversibility observed for the samples with $x = \frac{1}{2}$ and $\frac{2}{3}$ indicates that next-nearest-neighbor interactions also play an important role in determining the magnetic properties of these compounds.

INTRODUCTION

Until recently, our knowledge of the solid state chemistry of K_2NiF_4-type oxides was dominated by materials containing first-row transition elements. Only a few compounds which involved cations of metals from the second transition series were known, Sr_2RuO_4 being one example. This ruthenate was first prepared by Randall and Ward (1) and has subsequently been described as weakly metallic and paramagnetic down to 4.2 K (2). The solid solution $Sr_2Fe_xRu_{1-x}O_4$ ($0 \leq x \leq 0.5$) has also been reported, with a structural and magnetic study having been carried out using X-ray powder diffraction and Mössbauer spectroscopy (2). The iron and ruthenium ions in these phases were found to be randomly distributed over the octahedral B sites, with the iron substituting exclusively as Fe^{3+}, and the ruthenium consequently being oxidised to Ru^{5+}. The metallic band system of Sr_2RuO_4 was replaced by a localised electronic structure, with long-range antiferromagnetic order apparently present when $x = 0.5$. However, subsequent low-temperature neutron diffraction studies showed that, because of the competition between superexchange interactions of different signs and pathways, the sample with $x = 0.5$ was a spin glass rather than a Néel antiferromagnet (3). Similar frustrated magnetic properties have been observed in the related disordered material $Sr_3LaCuRu^{5+}O_8$ (4).

Systems containing Ru^{5+} ions are particularly interesting because the increased width of the $4d$ band, compared to that of the $3d$ band, together with the large correlation energy arising from half-filled t_{2g}^3 orbitals in octahedral coordination, will make the system suitable for a study of the competition between itinerant and localised electron behaviour. The present work was undertaken in order to investigate the change in the structural and magnetic properties of the solid solution $Sr_{3x}La_{2-3x}Zn_{1-x}Ru_xO_4$ ($\frac{1}{3} \leq x \leq \frac{2}{3}$) as a function of the Ru concentration. The sample with $x = \frac{1}{2}$ has been described previously as $Sr_3LaZnRuO_8$ (4). It was found that in this compound the Zn^{2+} and Ru^{5+} ions are disordered over the octahedral B sites of the K_2NiF_4 structure. The material is almost insulating and no magnetic Bragg scattering was observed in a neutron diffraction pattern collected at 1.5 K (4). The lack of long-range magnetic order in this material might be attributed to the fact that the magnetic concentration of the octahedral B sites (0.5) is smaller than the percolation threshold (0.59) for a nearest-neighbor (NN) square lattice (5). Thus long-range antiferromagnetic order might develop on increasing the Ru concentration. Alternatively, the high concentration of Ru^{5+} might lead to the formation of metallic band, as in the Ru^{4+} compound Sr_2RuO_4. The preparation of the new K_2NiF_4-type solid solution by direct solid state synthesis and the subsequent characterization of it by powder X-ray diffraction and magnetic measurements are described below.

EXPERIMENTAL

Polycrystalline samples of $Sr_{3x}La_{2-3x}Zn_{1-x}Ru_xO_4$ ($x = \frac{1}{3}$, 0.4, 0.5, 0.6, and $\frac{2}{3}$) were synthesised by firing pelletised stoichiometric mixtures of $SrCO_3$, dried La_2O_3 and RuO_2, and ZnO (Johnson Matthey Specpure reagents) in air at a temperature of 1100°C. The reactions took several days to complete and the reactants were periodically ground and repelletised during the heating process. The purity of

[1] To whom correspondence should be addressed.

0022-4596/94 $6.00

the resultant products was examined by powder X-ray diffraction using a Philips automated 1710 diffractometer operating with Cu$K\alpha$ radiation ($10° \leq 2\theta \leq 70°$).

Structural characterization of the materials was carried out using Rietveld refinement techniques with version 5.1 of the GSAS software package (6). Powder X-ray diffraction data were recorded in step scan mode at room temperature over the angular range $10° \leq 2\theta \leq 110°$, with a step size of 0.02° and a counting time of 10 seconds per point. The peak shape function was assumed to be of a pseudo-Voigt type (7), and the background level was fitted using a cosine Fourier series function with six refinable coefficients. Regions of the profile containing contributions from the aluminum sample plate were excluded from the refinements.

Electrical conductivity measurements were made on $Sr_2Zn_{1/3}Ru_{2/3}O_4$ in order to determine the position of this compound with respect to the localized/itinerant electron division. The measurements were carried out between 130 and 300 K using a standard 4-probe dc technique. Colloidal silver paint was used to attach metallic contacts to small, well-sintered ingots of the polycrystalline samples (ca. 2 × 2 × 10 mm), which were then mounted in an Oxford Instruments CF 200 cryostat. The temperature was measured with a rhodium–iron thermocouple. The distance between the voltage measuring probes was approximately 3 mm.

The dc molar magnetic susceptibilities of the samples with $x = \frac{1}{3}, \frac{1}{2}$, and $\frac{2}{3}$ were measured in magnetic fields of 1 and 5 kG over the temperature range $6 \text{ K} \leq T \leq 300$ K using a Cryogenic S600C SQUID magnetometer. The measurements were taken in a ^{4}He cryostat after cooling the sample in zero field (zfc) and after cooling in the measuring fields (fc). The temperature was controlled by a Lake Shore DRC-91C regulator using a gallium–aluminum–arsenide diode sensor. Samples were in the form of up to ca. 100 mg of finely ground powder, packed into a quartz tube. Values of the susceptibilities reported below have been corrected for the diamagnetic contributions of the constituent atoms and the sample container. For $Sr_2Zn_{1/3}Ru_{2/3}O_4$, the thermal remanent magnetization (TRM) was measured as a function of temperature after switching off an applied field of 1 kG in which the sample had previously been cooled. The magnetic hysteresis loop was also measured at 6 K in fields from 0 to 24 kG. In this case, the sample had been cooled in a magnetic field of 5 kG before the measurements were started.

RESULTS

Structural Characterisation

The powder X-ray diffraction patterns of all the samples studied could be indexed on the basis of the tetragonal K_2NiF_4 structure. No superlattice reflections which might be due to an ordered cation arrangement were detected in any of the phases investigated, and it was therefore concluded that the Zn^{2+} and Ru^{5+} ions are disordered over the octahedral sites, as in the case of $Sr_{1.5}La_{0.5}Zn_{0.5}Ru_{0.5}O_4$ (4). The refinement of 23 parameters in space group I4/mmm using 106 Bragg peaks converged to the structural parameters given in Table 1. In the case of samples with $x = 0.4, \frac{1}{2}, 0.6$, the refinements proved somewhat difficult because the intensity distribution and peak shape were ill defined, and this is reflected in the relatively high values of the intensity R factor (Table 1). In all cases, refinement of the occupancies for the oxygen and transition metal sites did not lead to any improvement in the overall fit, and the compounds were therefore assumed to be stoichiometric and to contain only pentava-

TABLE 1
Structural Parameters for $Sr_{3x}La_{2-3x}Zn_{1-x}Ru_xO_4$ ($\frac{1}{3} \leq x \leq \frac{2}{3}$) at Room Temperature

x		$\frac{1}{3}$	0.4	$\frac{1}{2}$	0.6	$\frac{2}{3}$
Lattice parameters	a (Å)	3.9217(1)	3.9207(1)	3.9294(1)	3.9204(1)	3.9248(1)
	c (Å)	12.7407(2)	12.7063(2)	12.6214(4)	12.6317(2)	12.6053(2)
	Sr/La z	0.3592(1)	0.3587(1)	0.3555(1)	0.3563(1)	0.3547(1)
	B_{iso} (Å^2)	0.31(2)	0.21(3)	0.40(4)	0.58(3)	0.37(2)
	Zn/Ru					
	B_{iso} (Å^2)	0.12(3)	0.10(4)	0.68(6)	0.47(4)	0.02(3)
	O1 z	0.1720(5)	0.1664(6)	0.1727(7)	0.1594(5)	0.1640(4)
	B_{iso} (Å^2)	1.1(1)	0.6(2)	2.8(2)	1.2(1)	0.7(1)
	O2					
	B_{iso} (Å^2)	0.5(1)	0.4(2)	2.1(2)	0.2(1)	0.2(1)
R factors	R_{wp} (%)	11.7	15.6	14.9	14.3	11.1
	R_p (%)	8.1	11.6	11.0	11.0	7.3
	R_I (%)	5.1	8.9	8.7	8.3	4.7

Note. Space Group: *I4/mmm* Sr/La on 4*e* (0 0 z), Zn/Ru on 2*a* (0 0 0), O1 on 4*e* (0 0 z), O2 on 4*c* ($\frac{1}{2}$ 0 0).

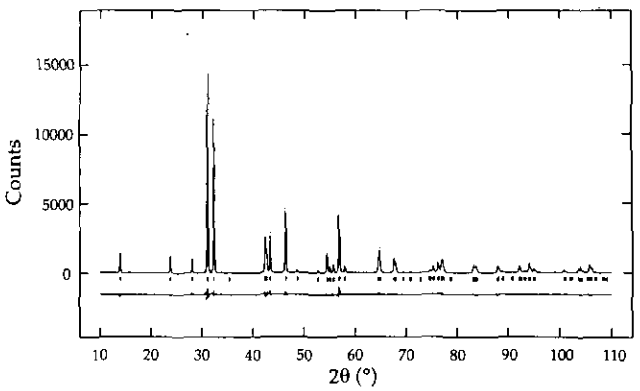

FIG. 1. The observed (points), calculated (solid line), and difference (below) X-ray diffraction profiles for $SrLaZn_{2/3}Ru_{1/3}O_4$. Reflection positions are marked.

lent Ru. Typical observed, calculated, and difference diffraction profiles are drawn in Fig. 1. The resultant bond distances are presented in Table 2. The variation of the lattice parameters, unit cell volume, and the *c*/*a* ratio is plotted as a function of the Ru concentration, *x*, in Fig. 2.

Electrical Measurements

The results of resistivity measurements on $Sr_2Zn_{1/3}Ru_{2/3}O_4$ are shown in Fig. 3a. The temperature variation of the resistivity of $Sr_{1.5}La_{0.5}Zn_{0.5}Ru_{0.5}O_4$ is also plotted in order to show the effect of the Ru/Zn ratio on the electrical properties. The Ru-rich material is found to be a semiconductor, and the magnitude of its resistivity is markedly reduced compared to that of $Sr_{1.5}La_{0.5}Zn_{0.5}Ru_{0.5}O_4$. Attempts to account for the observed data in terms of a simple Arrhenius model were unsuccessful, as were those based on a small polaron model. In view of the fact that the Mott variable-range hopping (VRH) mechanism has been observed in many perovskite-related phases (8–10), a least-squares fit of the data to the following equation was carried out:

$$\rho = \rho_0(T/T_0)^{1/2} \exp[(T_0/T)^{\nu}].$$

TABLE 2
Selected Bond Lengths (Å) in $Sr_{3x}La_{2-3x}Zn_{1-x}Ru_xO_4$ ($\frac{1}{3} \le x \le \frac{2}{3}$) at Room Temperature

x	$\frac{1}{3}$	0.4	$\frac{1}{2}$	0.6	$\frac{2}{3}$
Zn/Ru–O1 (×2)	2.191(6)	2.115(7)	2.179(9)	2.014(7)	2.068(5)
Zn/Ru–O2 (×4)	1.961(1)	1.960(1)	1.965(1)	1.960(1)	1.962(1)
Mean Zn/Ru–O	2.038	2.012	2.036	1.978	1.997
Sr/La–O1	2.385(6)	2.443(7)	2.307(9)	2.488(7)	2.404(5)
Sr/La–O1′ (×4)	2.801(1)	2.791(1)	2.801(1)	2.779(1)	2.785(1)
Sr/La–O2 (×4)	2.658(1)	2.659(1)	2.681(1)	2.671(1)	2.684(1)
Mean Sr/La–O	2.691	2.694	2.693	2.699	2.698

Note. O1′ at $(\frac{1}{2}, \frac{1}{2}, \frac{1}{2} - z)$.

Excellent agreement was obtained between experiment and theory although, due to the limited temperature range over which the experiment was performed, the data were relatively insensitive to the value of ν and we were therefore unable to distinguish between 2D VRH ($\nu = 3$) and 3D VRH ($\nu = 4$). Figure 3b shows the plot of $\ln(\rho T^{-1/2})$ versus $T^{-1/3}$ which is appropriate for the 2D case. Data analysis using the Shklovskii–Efros model with $\nu = \frac{1}{2}$ (11) was less successful than the analysis described above.

Magnetic Measurements

The temperature dependence of the molar magnetic susceptibility of $SrLaZn_{2/3}Ru_{1/3}O_4$, measured in applied fields of 1 and 5 kG, is shown in Fig. 4. The zfc and fc curves overlay each other throughout the experimental temperature range (Fig. 4a) and the data obey a Curie–Weiss law above ca. 150 K with the Weiss tempera-

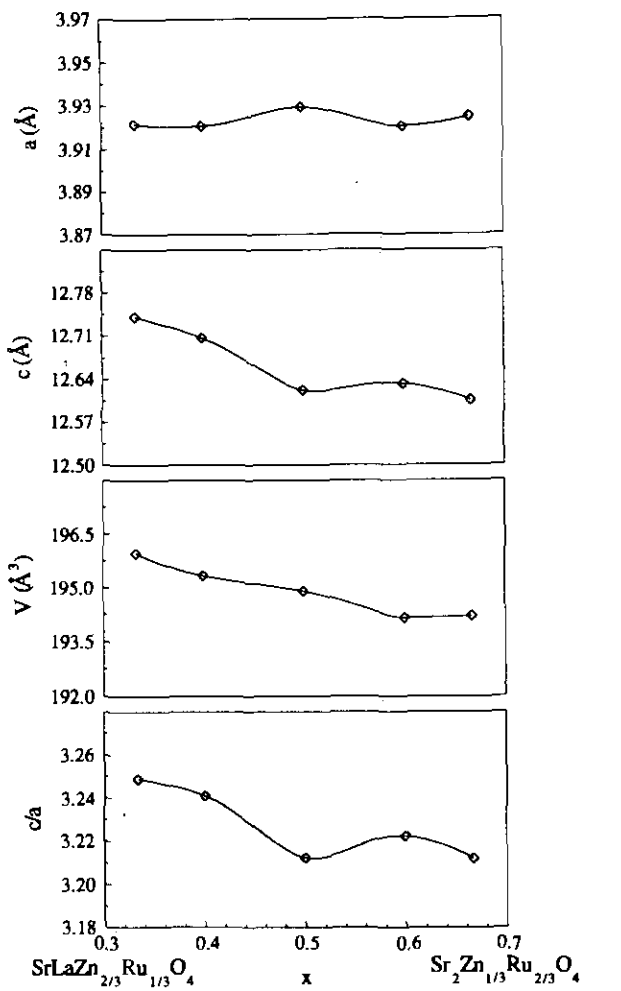

FIG. 2. Variation of lattice parameters *a* and *c*, unit cell volume *V*, and ratio *c*/*a* for the series $Sr_{3x}La_{2-3x}Zn_{1-x}Ru_xO_4$ ($0 \le x \le \frac{2}{3}$).

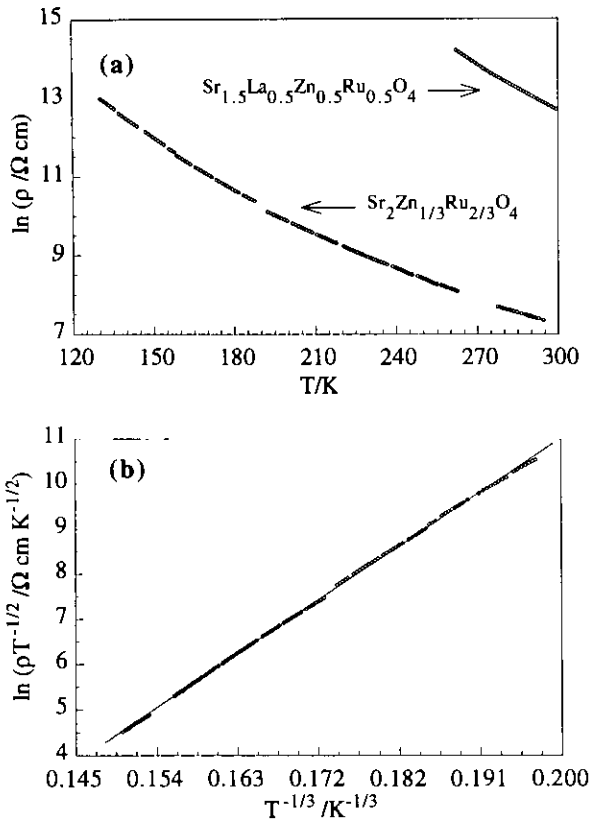

FIG. 3. (a) The resistivity of $Sr_2Zn_{1/3}Ru_{2/3}O_4$ as a function of temperature. For comparison the resistivity data of $Sr_{1.5}La_{0.5}Zn_{0.5}Ru_{0.5}O_4$ are also plotted. (b) The linear fit for a 2D VRH mechanism.

ture of -75 K. However, below this temperature there is a progressive deviation from simple paramagnetic behavior (Fig. 4b). An effective magnetic moment of 3.49 μ_B per Ru^{5+} ion can be deduced from the data in the high temperature region.

Figure 5a shows the zfc and fc molar magnetic susceptibilities of the $x = \frac{1}{2}$ sample, $Sr_{1.5}La_{0.5}Zn_{0.5}Ru_{0.5}O_4$, as a function of temperature. No prominent peak in the susceptibility, characteristic of long-range antiferromagnetism, was observed over the whole temperature range. However, the data measured in an applied field of 1 kG show a slight divergence between the zfc and fc curves in the temperature range 20 K $< T <$ 150 K, indicating that short-range interactions are causing the formation of spin clusters. This magnetic irreversibility is suppressed as the applied field is increased; the zfc and fc data measured in 5 kG overlay each other to the lowest temperature measured. The temperature dependence of the inverse zfc molar susceptibility, measured in an applied field of 1 kG, is also plotted in Fig. 5b. The susceptibility data begin to depart from Curie–Weiss behavior at ca. 200 K, and show a marked deviation below ca. 20 K. Analysis of the high temperature data leads to $\mu_{eff} = 3.36\ \mu_B$ per Ru^{5+} ion and $\theta = -124$ K.

The magnetic properties of $Sr_2Zn_{1/3}Ru_{2/3}O_4$ were found to be more complex than those described above. The results of magnetic susceptibility measurements on this material are shown in Fig. 6. The zfc and fc curves agree well down to $T \approx 10$ K at which temperature the zfc data exhibit a sharp cusp. However, below this point the fc curve continues to increase, albeit at a slower rate, whereas the zfc susceptibility decreases as the sample is cooled further. Unusual, field-dependent magnetic behavior is also observed with the magnitude of the fc susceptibility below T_f being reduced when the applied field is increased from 1 to 5 kG. The observation of a thermoremanent magnetization (TRM) is evidence of frustrated magnetism; the TRM decays rapidly with increasing temperature and vanishes at ~10 K (Fig. 6a). As depicted in Fig. 6b, the magnetic susceptibility does not follow a Curie–Weiss law in any part of the temperature range over which the data were collected. Attempts to model the data at $T > 150$ K led to the very large values for both the effective magnetic moment (4.4 μ_B per Ru^{5+} ion) and the Weiss constant (-1060 K). The fc hysteresis loop, obtained by cooling the sample 5 kG from room temperature to 6 K, is presented in Fig. 6c. The observed

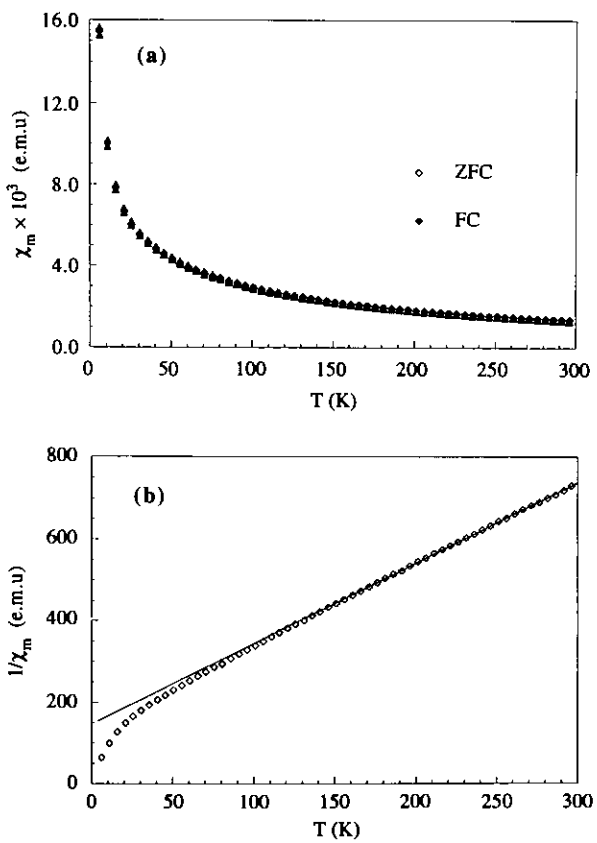

FIG. 4. (a) The temperature dependence of the (superimposable) zfc and fc molar magnetic susceptibilities of $SrLaZn_{2/3}Ru_{1/3}O_4$ measured in fields of 1 kG (diamond) and 5 kG (triangles). (b) The inverse zfc susceptibility of $SrLaZn_{2/3}Ru_{1/3}O_4$ in a field of 1 kG.

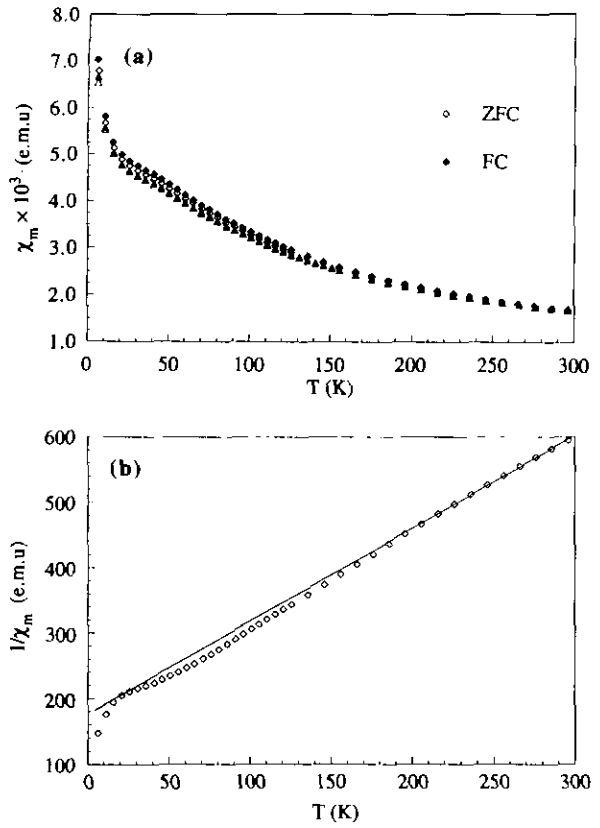

FIG. 5. (a) The temperature dependence of the zfc and fc molar magnetic susceptibilities of $Sr_{1.5}La_{0.5}Zn_{0.5}Ru_{0.5}O_4$ in fields of 1 kG (diamond) and 5 kG (triangles). (b) The inverse zfc susceptibility of $Sr_{1.5}La_{0.5}Zn_{0.5}Ru_{0.5}O_4$ measured in a field of 1 kG.

loop is slightly asymmetrical and shifted from the origin, as is often the case in spin glasses below T_f (12, 13).

DISCUSSION

The structural variation of the compounds $Sr_{3x}La_{2-3x}Zn_{1-x}Ru_xO_4$ with the Ru^{5+} content, x, is rather complex, as might have been expected on the grounds that the substitution of Zn^{2+} by the smaller Ru^{5+} on the B sites is accompanied by the replacement of La^{3+} by the larger Sr^{2+} (14). The substitution of Zn^{2+} by Ru^{5+} thus might be expected to reduce the lengths of the Zn/Ru–O1 and the Zn/Ru–O2 bonds. Examination of the data in Table 2 shows that neither reduction occurs as a smooth function of composition, but that there is a general downward trend in the Zn/Ru–O1 distance as x decreases. However, the Zn/Ru–O2 distance is effectively constant across the whole composition range. The absence of a smooth trend in the axial Zn/Ru–O1 distance may be due in part to the failure to locate the O1 atom accurately in X-ray diffraction experiments, but the lack of variation in the Zn/Ru–O2 distance is likely to be a real effect because it depends only on the value of the unit cell parameter, a, both atoms being on a special position of space group $I4/mmm$. This near constancy can be understood by taking into account the fact that any reduction in the Zn/Ru–O2 distance, that is a decrease in the unit cell parameter, would tend to shorten the Sr/La–O1′ distance whereas the increase in Ru content is accompanied by an increase in Sr content and hence an increase in the Sr/La–O1′ distance is expected. Thus, an increase in the Ru content produces conflicting structural requirements for the lengths of the bonds which lie parallel to, or approximately parallel to, the xy plane. The structure has more freedom along the c axis and the requirements of the Zn/Ru site are met by a reduction of the c parameter, and a small shift in the fractional coordinates of O1 and Sr/La sites

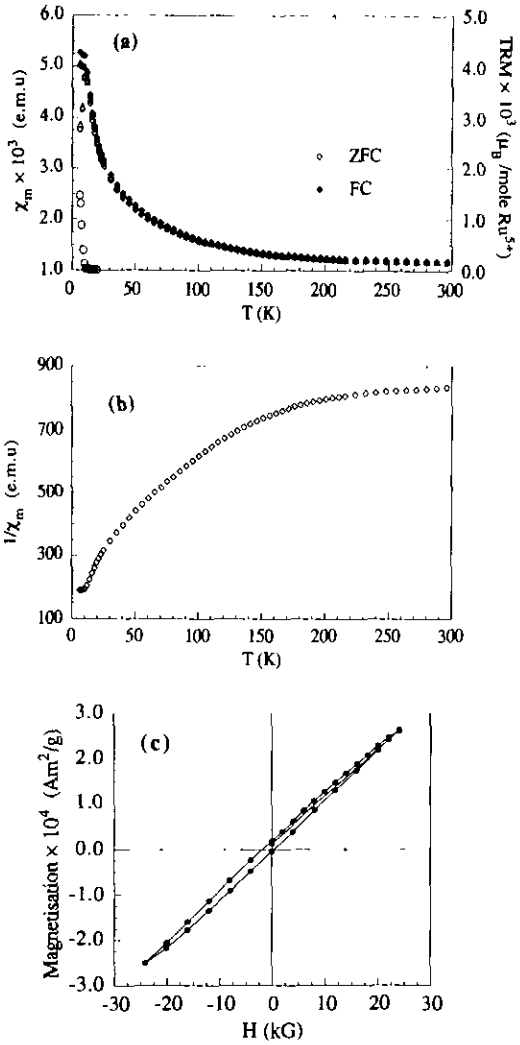

FIG. 6. (a) The temperature dependence of the zfc and fc molar magnetic susceptibilities of $Sr_2Zn_{1/3}Ru_{2/3}O_4$ in fields of 1 kG (diamonds) and 5 kG (triangles). The thermoremanent magnetization (circles) is also shown. (b) The temperature dependence of the zfc inverse susceptibility of $Sr_2Zn_{1/3}Ru_{2/3}O_4$ in a magnetic field of 1 kG. (c) FC magnetic hysteresis loop of $Sr_2Zn_{1/3}Ru_{2/3}O_4$ at $T = 6$ K.

such that the Zn/Ru–O1 distance shows a general decrease as x increases. However, the expected increase in the Sr/La–O1 distance is not observed, and any interpretation of the structural data other than the Zn/Ru–O2 bond distance should not be overemphasized. The unit cell parameters of $Sr_{1.5}La_{0.5}Zn_{0.5}O_4$ are anomalous with respect to all the other compositions, and this compound also has unusually high-temperature factors for atoms O1 and O2 (Table 1). These anomalies may indicate that some form of short-range cation ordering is present in this sample, although it cannot be accurately characterized by standard X-ray (or neutron) powder diffraction techniques. The absence of long-range cation ordering found in the compounds under discussion is perhaps not surprising since the layered character of the K_2NiF_4 structure will effectively insulate the perovskite-like slabs and significantly reduce the ordering energy that arises from the size and charge differences of the B cations. To date, only a few K_2NiF_4-type oxides have been reported to have an ordered cation arrangement, e.g., $La_2Li_{0.5}Co_{0.5}O_4$ (15).

The results of our electrical measurements (Fig. 3) indicate that $Sr_2Zn_{1/3}Ru_{2/3}O_4$ is a semiconductor, but with a much lower resistivity ($\rho_{295\ K}$ = 1.6 kΩ cm) than $Sr_{1.5}La_{0.5}Zn_{0.5}Ru_{0.5}O_4$ ($\rho_{295\ K}$ = 0.40 MΩ cm). This result can be easily understood because the former compound contains a higher concentration of Ru^{5+}, and thus more potential charge carriers, than the latter. However, the value of the resistivity is still considerably higher than that expected for a system which can be described by a delocalised electron model. This is presumably because the large correlation energy associated with t_{2g}^3 electron configuration of octahedral Ru^{5+} dominates over the increased width of 4d band and ensures that the electrons in t_{2g} band remain localized. The K_2NiF_4-type first-row transition metal oxides with half-filled t_{2g}^3 orbitals, i.e., Ca_2MnO_4 and $LaSrCrO_4$, are also good insulators (16, 17). The observed VRH behavior is consistent with the presence of structural disorder in this compound. Such site disorder will create a random field, and accordingly lead to Anderson localisation at the band edges (8). Figure 3b shows that a model based on 2D hopping behavior gives excellent agreement with the experimental data. However, the electrical resistivity data were collected on a polycrystalline sample and they will inevitably contain contributions from the grain boundaries. The thermopower measurements that can disentangle these effects were not performed and the dimensionality of the hopping process cannot therefore be deduced unambiguously from our results, particularly in view of the limited temperature range of the data, which was referred to above.

The magnetic properties of $SrLaZn_{2/3}Ru_{1/3}O_4$ are typical of a magnetically dilute system (18). The material is essentially paramagnetic, but with the presence of short-range magnetic interactions at low temperatures. No irreversibility is observed between the zfc and fc data throughout the measured temperature range (Fig. 4a), nor does the susceptibility show any field dependence. The effective magnetic moment (3.49 μ_B) deduced from the high temperature data is in the range expected for a localized t_{2g}^3 orbital and suggests that the Ru^{5+} ions in this compound can be considered to lie within the localised electron regime. The progressive deviation from Curie–Weiss behavior suggests that relatively strong short-range magnetic interactions occur between the Ru^{5+} ions below ca. 150 K (Fig. 4b). The Weiss temperature of −75 K indicates that these interactions are antiferromagnetic in nature, as would be predicted by superexchange theory (19). The site percolation on a 24 × 24 square lattice is illustrated for $x = \frac{1}{3}$, $\frac{1}{2}$, and $\frac{2}{3}$ in Fig. 7. If NN interactions alone are significant, the infinite 'percolating' cluster that permits long-range magnetic order can only be achieved if $x > 0.59$. The concentration of magnetic Ru^{5+} ions in $SrLaZn_{2/3}Ru_{1/3}O_4$ is thus well below the percolation limit for a NN square lattice, and the absence of long-range magnetic order is to be expected. A similar lack of ordering has been observed for small values of x in the solid solutions $LaSrAl_{1-x}Fe_xO_4$ and $K_2Mg_{1-x}Mn_xF_4$ (20, 21). If NNN interactions are also significant, the critical concentration drops to 0.29, and $SrLaZn_{2/3}Ru_{1/3}O_4$ is then slightly above the percolation threshold. However, the two types of interaction may compete rather than reinforce each other, a point that we shall return to below.

$Sr_{1.5}La_{0.5}Zn_{0.5}Ru_{0.5}O_4$ does not show (4) magnetic Bragg scattering in the neutron diffraction pattern collected at

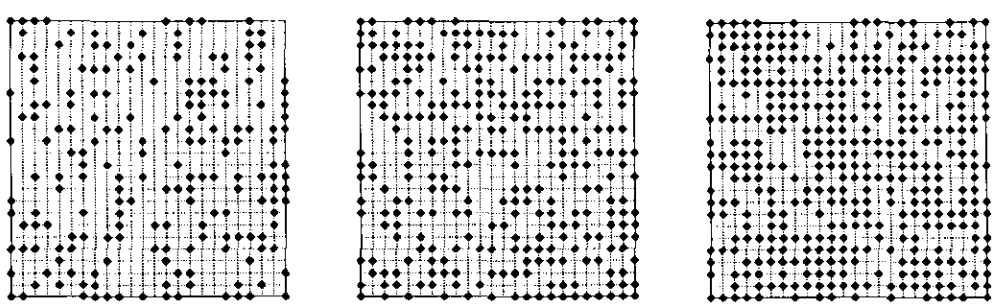

FIG. 7. Site percolation on a 24 × 24 square lattice for (a) $x = \frac{1}{3}$; (b) $x = \frac{1}{2}$; and (c) $x = \frac{2}{3}$. Occupied sites are shown as dots.

1.5 K. The magnetic measurements performed in this study are consistent with this result; there is no apparent cusp in the susceptibility which might be taken as evidence for long-range antiferromagnetic order. The magnetic behavior of this compound may thus be described in terms of percolation theory; as the concentration of Ru^{5+} (0.5) is smaller than the NN percolation threshold (0.59), no long-range magnetic order is developed. However, if next nearest neighbor (NNN) interactions are also considered, the magnetic concentration in the present compound is significantly above the percolation limit (0.29 for a square lattice), and long-range magnetic order might be expected to develop at very low temperatures. It has been shown that superexchange interactions via Ru–O–O–Ru pathways (i.e., the NNN pathway in a K_2NiF_4 structure) are strong enough to give rise to long-range antiferromagnetic order at $T_N \approx 23$ K in the ordered perovskite Sr_2YRuO_6 (22), and they are, therefore, likely to be significant at a similar temperature in $Sr_{1.5}La_{0.5}Zn_{0.5}Ru_{0.5}O_4$. Nevertheless, neutron diffraction experiments show that this compound is not magnetically ordered at a temperature of 1.5 K. This is probably because the strong antiferromagnetic NNN Ru–O–O–Ru superexchange interactions will compete with the NN Ru–O–Ru interactions, thus introducing a certain degree of spin frustration. It has been shown (3, 23) that such magnetic frustration in perovskite-related compounds can often destroy long-range magnetic order and lead to the formation of a spin glass phase. Hence, $Sr_{1.5}La_{0.5}Zn_{0.5}Ru_{0.5}O_4$ is likely to behave as a spin glass at very low temperatures rather than as a dilute magnetic system; clusters created by antiferromagnetic short-range interactions will grow in size with decreasing temperature, causing the susceptibility to deviate from the Curie–Weiss Law. We would predict that at $T_f < 6$ K a cluster of infinite size is formed, but that the development of long-range magnetic order is frustrated (24). If we are correct, the susceptibility will have a cusp at low temperatures and will show a marked hysteresis below that point. It should be noted that the temperature at which the deviation from the Curie–Weiss Law begins (ca. 200 K) and the value of the Weiss temperature are larger in the case of $Sr_{1.5}La_{0.5}Zn_{0.5}Ru_{0.5}O_4$ than they were in that of $SrLaZn_{2/3}Ru_{1/3}O_4$. This result, together with a slightly reduced effective magnetic moment (3.36 μ_B, compared to 3.49 μ_B for $x = \frac{1}{3}$), indicates that the extent of antiferromagnetic clustering is enhanced in $Sr_{1.5}La_{0.5}Zn_{0.5}Ru_{0.5}O_4$. Nonetheless, the value of μ_{eff} is still in good agreement with the expected value for a localized t_{2g}^3 configuration. The high temperature clusters are likely to carry an uncompensated magnetic moment, the orientation of which will be influenced by an external field. The small divergence between the zfc and fc susceptibilities observed in 1 kG at $T < \sim 160$ K can be attributed to such an effect. Upon increasing the applied field from 1 to 5 kG, the fc susceptibility is suppressed, as is often observed in frustrated magnetic systems (25). It should be noted, however, that field-dependent behaviour is also observed (Fig. 5) in the zfc susceptibility below 160 K. This could be due to the presence of a small amount of ferromagnetic $SrRuO_3$, the Curie temperature of which is known to be 160 ± 10 K (26). Alternatively, finite clusters with antiferromagnetic interactions may behave as superparamagnetic particles in this temperature range.

The magnetic susceptibility of $Sr_2Zn_{1/3}Ru_{2/3}O_4$ reveals a more complex temperature dependence. As shown in Fig. 6a, while the zfc curve appears to have a maximum at ca. 10 K, the fc susceptibility continues to increase with decreasing temperature. Such magnetic irreversibility is typical of a frustrated magnetic system, for example a spin glass (27). This indicates that, as described above, the competition between the NN and NNN interactions produces a substantial degree of frustration in this compound. However, unlike $Sr_{1.5}La_{0.5}Zn_{0.5}Ru_{0.5}O_4$, no divergence of the zfc and fc data is observed at temperatures above the freezing temperature, T_f. An increase in the fc susceptibility below T_f has previously been observed in some spin glasses and has been ascribed to the presence of a small number of unfrozen spins which experience a net internal field of zero (28). These entropic clusters will then contribute a paramagnetic component to the overall magnetic susceptibility. The field dependence of the fc data at $T < T_f$ also demonstrates the frustrated nature of $Sr_2Zn_{1/3}Ru_{2/3}O_4$. As the applied field is increased from 1 to 5 kG, the magnitude of the fc data is slightly reduced. This is presumably because, when an external field is applied to spin glasses, the random interactions compete with the Zeeman energy and can be significantly reduced by a strong field (27). The magnetic irreversibility is again confirmed by the observation of a thermoremanent magnetization (TRM). It may be noted that the behavior of the TRM is similar to the linear dependence often identified in metallic spin glasses (29). Levy *et al.* suggested that in spin glasses correlations among the spin directions and local anisotropy fields might produce a macroscopic anisotropy during field-cooling (30), resulting in a displaced hysteresis loop. Figure 6c shows that the fc hysteresis curve is indeed shifted from the origin although the shift is less prominent than those observed previously in other oxide spin glasses (13, 23). In fact, the frustrated magnetic behavior discussed above is not only associated with spin glasses. There exist a number of frustrated magnetic systems which retain long-range magnetic order at low temperatures (31). In view of the high concentration of Ru^{5+} ions, $Sr_2Zn_{1/3}Ru_{2/3}O_4$ may contain a backbone of spins which show long range magnetic order below ca. 10 K. It is surprising that the susceptibility of $Sr_2Zn_{1/3}Ru_{2/3}O_4$ does not follow a Curie–Weiss law in any part of the experimental temperature range (Fig. 6b). The magnetic susceptibility is nearly temperature-independent at high

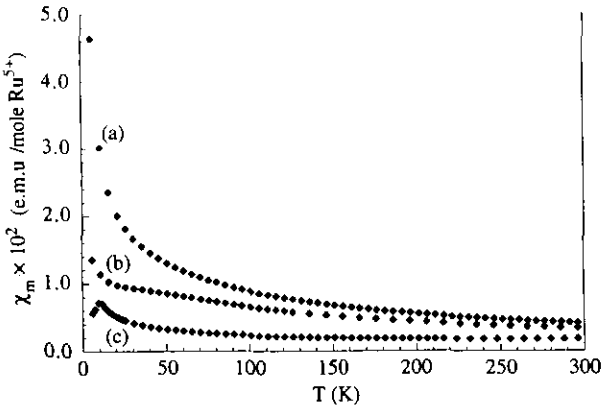

FIG. 8. The zfc molar magnetic susceptibility of $Sr_{3x}La_{2-3x}Zn_{1-x}Ru_xO_4$ as a function of temperature, collected in an applied field of 1 kG. (a) $x = \frac{1}{3}$; (b) $x = \frac{1}{2}$; (c) $x = \frac{2}{3}$.

temperatures, as in metallic Sr_2RuO_4 (1, 2). Figure 8 also shows that the high temperature susceptibility (per Ru^{5+} mole) of $Sr_2Zn_{1/3}Ru_{2/3}O_4$ is considerably smaller than those of the samples with $x = \frac{1}{3}$ and $\frac{1}{2}$. One possible explanation is that in this compound the relatively high concentration of NN Ru^{5+} gives the 4*d* band a significant width, and a degree of electron delocalization is thus introduced. This itinerant electron character is reflected in the high values of μ_{eff} and θ, as it was in the case of the 3D perovskite Ba_2LaRuO_6 (32). Although the interatomic interactions in these compounds are strong enough to move the magnetic properties away from the localized-electron limit, the Hubbard splitting remains strong enough for the electrical conductivity to retain an activation energy. In the case of $Sr_2Zn_{1/3}Ru_{2/3}O_4$, the insulating nature of the compound may be enhanced by the low dimensionality of the crystal structure.

To summarise, although previous studies have shown that the magnetic properties of the K_2NiF_4-type oxides are dominated by nearest-neighbor interactions, the work presented in this paper reveals the importance of next-nearest-neighbor interactions. Our results suggest that the electronic properties of Ru^{5+} in the solid solution $Sr_{3x}La_{2-3x}Zn_{1-x}Ru_xO_4$ span the whole spectrum between isolated, localized electron configurations ($x = \frac{1}{3}$) and the itinerant electron limit ($x = \frac{2}{3}$). Clearly, further work needs to be carried out in order to fully understand the electronic properties of these materials.

ACKNOWLEDGMENTS

S.H.K. is grateful to ICI for the award of a Scholarship. The SQUID magnetometer used in this work was bought with the help of the SERC.

REFERENCES

1. J. J. Randall and R. Ward, *J. Am. Chem. Soc.* **81,** 2629 (1959).
2. R. Greatrex, N. N. Greenwood, and M. Lal, *Mater. Res. Bull.* **15,** 113 (1980).
3. P. D. Battle, S. K. Bollen, and A. V. Powell, *J. Solid State Chem.* **99,** 267 (1992).
4. M. P. Attfield, P. D. Battle, S. K. Bollen, S. H. Kim, A. V. Powell, and M. Workman, *J. Solid State Chem.* **96,** 344 (1992).
5. C. Domb and N. W. Dalton, *Proc. Phys. Soc.* **89,** 856 (1966).
6. A. C. Larson and R. B. Von Dreele, "General Structure Analysis System (GSAS)." Los Alamos National Laboratory Report, LAUR 86-748, 1990.
7. C. J. Howard, *J. Appl. Crystallogr.* **15,** 615 (1982).
8. N. F. Mott and E. A. Davis, "Electronic Processes in Non-Crystalline Materials," 2nd ed. Oxford Univ. Press, London, 1979.
9. M. A. Kastner, R. J. Birgeneau, C. Y. Chen, Y. M. Chiang, D. R. Gabbe, H. P. Jenssen, T. Junk, C. J. Peters, P. J. Picone, Tineke Thio, T. R. Thurston, and H. L. Tuller, *Phys. Rev. B* **37,** 111 (1988).
10. T. J. Goodwin, H. B. Radousky, and R. N. Shelton, *Physica C* **204,** 212 (1992).
11. A. L. Efros and B. I. Shklovskii, *J. Phys. C: Solid State Phys.* **8,** L45 (1975).
12. W. Abdul-Razzaq, *Phys. Rev. B* **39,** 9719 (1989).
13. N. Ali, P. Hill, X. Zhang, and F. Willis, *J. Alloys Compounds* **181,** 281 (1992).
14. R. D. Shannon, *Acta Crystallogr. Sect. A* **32,** 751 (1976).
15. G. Demazeau, M. Pouchard, M. Thomas, J. F. Colombet, J. C. Grenier, L. Fournes, J. L. Soubeyroux, and P. Hagenmuller, *Mater. Res. Bull.* **15,** 451 (1980).
16. D. E. Cox, G. Shirane, R. J. Birgeneau, and J. B. MacChesney, *Phys. Rev.* **188,** 930 (1969).
17. G. LeFlem, G. Demazeau, and P. Hagenmuller, *J. Solid State Chem.* **44,** 82 (1982).
18. R. B. Stinchcombe, in "Phase Transitions and Critical Phenomena" (C. Domb and M. S. Green, Ed.), Vol. 7. Academic Press, London, 1983.
19. J. B. Goodenough, "Magnetism and the Chemical Bond," Wiley, New York, 1963.
20. P. Ganguly and C. N. R. Rao, *J. Solid State Chem.* **53,** 14 (1984).
21. D. J. Breed, K. Gilijames, J. W. E. Sterkenburg, and A. R. Miedema, *J. Appl. Phys.* **41,** 1267 (1970).
22. P. D. Battle and W. J. Macklin, *J. Solid State Chem.* **52,** 138 (1984).
23. R. Rodríguez, A. Fernández, A. Isalgué, J. Rodríguez, A. Labarta, J. Tejada, and X. Obradors, *J. Phys. C: Solid State Phys.* **18,** L401 (1985).
24. M. Cyrot, *Solid State Commun.* **39,** 1009, (1981).
25. A. Labarta, R. Rodríguez, L. Balcells, J. Tejada, X. Obradors, and F. J. Berry, *Phys. Rev. B* **44,** 691 (1991).
26. A. Callaghan, C. W. Moeller, and R. Ward, *Inorg. Chem.* **5,** 1572 (1966).
27. K. Binder and A. P. Young, *Rev. Mod. Phys.* **58,** 801 (1986).
28. D. Fiorani, S. Viticoli, J. L. Dormann, J. L. Tholence, and A. P. Murani, *Phys. Rev. B* **30,** 2776 (1984).
29. S. Oseroff, and F. G. Gandra, *J. Appl. Phys.* **61,** 3421 (1985).
30. P. M. Levy, C. Morgan-Pond, and A. Fert, *J. Appl. Phys.* **53,** 2168 (1982).
31. M. P. Attfield, P. D. Battle, S. K. Bollen, T. C. Gibb, and R. J. Whitehead, *J. Solid State Chem.* **100,** 37 (1992).
32. P. D. Battle, J. B. Goodenough, and R. Price, *J. Solid State Chem.* **46,** 234 (1983).